Identification of two classes of somatosensory neurons that display resistance to retrograde infection by rabies virus

Albisetti, Gioele W ; Ghanem, Alexander ; Foster, Edmund ; Conzelmann, Karl-Klaus ; Zeilhofer, Hanns Ulrich ; Wildner, Hendrik

Abstract: Glycoprotein-deleted (ΔG) rabies virus-mediated monosynaptic tracing has become a standard method for neuronal circuit mapping, and is applied to virtually all parts of the rodent nervous system including the spinal cord and primary sensory neurons. Here we identified two classes of unmyelinated sensory neurons (non-peptidergic/NP- and C-LTMR/TH neurons) that are resistant to direct and transsynaptic infection from the spinal cord with rabies viruses carrying glycoproteins in their envelopes that are routinely used for infection of CNS neurons (SAD-G or N2C-G). However, the same neurons were susceptible to infection with EnvA-pseudotyped rabies virus in TVA transgenic mice, indicating that resistance to retrograde infection was due to impaired virus adsorption rather than to deficits in subsequent steps of infection. These results demonstrate an important limitation of rabies virus-based retrograde tracing of sensory neurons in adult mice, and may help to better understand the molecular machinery required for rabies virus spread in the nervous system. In this study mice of both sexes were used.SIGNIFICANCE STATEMENTIn order to understand the neuronal bases of behavior it is important to identify the underlying neural circuitry. Rabies virus based monosynaptic tracing has been used to identify neuronal circuits in various parts of the nervous system. This has included connections between peripheral sensory neurons and their spinal targets, which form the first synapse in the somatosensory pathway. Here we demonstrate that two classes of unmyelinated sensory neurons, which account for more than 40% of DRG neurons, display resistance to rabies infection. Our results are therefore critical for interpreting monosynaptic rabies-based tracing in the sensory system. In addition, identification of rabies resistant neurons might provide a means for future studies addressing rabies pathobiology.

DOI: https://doi.org/10.1523/JNEUROSCI.1277-17.2017

JNeurosci
THE JOURNAL OF NEUROSCIENCE

Research Articles: Systems/Circuits

Identification of two classes of somatosensory neurons that display resistance to retrograde infection by rabies virus

Gioele W. Albisetti[1], Alexander Ghanem[2], Edmund Foster[1], Karl-Klaus Conzelmann[2], Hanns Ulrich Zeilhofer[1,3] and Hendrik Wildner[1]

[1]*Institute of Pharmacology and Toxicology, University of Zurich, Winterthurerstrasse 190, CH-8057 Zürich, Switzerland*

[2]*Max von Pettenkofer Institute & Gene Center, Virology, Faculty of Medicine, LMU München, Feodor-Lynen-Str. 25, 81377 München, Germany*

[3]*Institute of Pharmaceutical Sciences, Swiss Federal Institute (ETH) Zurich, Wolfgang-Pauli Strasse, CH-8090 Zürich, Switzerland*

DOI: 10.1523/JNEUROSCI.1277-17.2017

Received: 9 May 2017

Revised: 29 August 2017

Accepted: 11 September 2017

Published: 26 September 2017

Author contributions: GA performed virus injections and performed and analyzed morphological experiments. K.K.C. and A.G. produced and provided the majority of pseudotyped G-deleted rabies viruses used in this study. EF performed virus injections. HW analyzed experiments. H.W. and H.U.Z. designed experiments and wrote the manuscript. All authors have commented on the manuscript.

Conflict of Interest: The authors declare no competing financial interests.

This work was supported by an ERC Advanced Investigator Grant (DHISP 250128), a grant from the Swiss National Research Foundation (156393) and a Wellcome Trust Collaborative Award in Science (200183/Z/15/Z) (to H.U.Z.). HW was supported by the Olga Mayenfisch foundation. KKC and AG were supported by DFG SFB870 (KKC) and LMUexcellent and LMU WiFoMed (AG).

Correspondence: Dr Hendrik Wildner, Institute of Pharmacology and Toxicology, University of Zurich, Winterthurerstrasse 190, CH-8057 Zurich, Switzerland, Tel. +41 44 63 55938, hwildner@pharma.uzh.ch

Cite as: J. Neurosci ; 10.1523/JNEUROSCI.1277-17.2017

Identification of two classes of somatosensory neurons that display resistance to retrograde infection by rabies virus

DRG neuron subsets resistant to rabies infection

[1]Gioele W. Albisetti, [2]Alexander Ghanem, [1]Edmund Foster [2]Karl-Klaus Conzelmann, [1,3]Hanns Ulrich Zeilhofer, [1]Hendrik Wildner

[1]Institute of Pharmacology and Toxicology, University of Zurich, Winterthurerstrasse 190, CH-8057 Zürich, Switzerland
[2]Max von Pettenkofer Institute & Gene Center, Virology, Faculty of Medicine, LMU München, Feodor-Lynen-Str. 25, 81377 München, Germany[3]Institute of Pharmaceutical Sciences, Swiss Federal Institute (ETH) Zurich, Wolfgang-Pauli Strasse, CH-8090 Zürich, Switzerland

Correspondence: Dr Hendrik Wildner
Institute of Pharmacology and Toxicology
University of Zurich
Winterthurerstrasse 190
CH-8057 Zurich
Switzerland
Tel. +41 44 63 55938
hwildner@pharma.uzh.ch

Number of pages: 16
Number of figures: 7
Number of words for Abstract (161), Introduction (622), and Discussion (1386)
Conflict of Interest: There is no conflict of interest
Acknowledgements:

This work was supported by an ERC Advanced Investigator Grant (DHISP 250128), a grant from the Swiss National Research Foundation (156393) and a Wellcome Trust Collaborative Award in Science (200183/Z/15/Z) (to H.U.Z.). HW was supported by the Olga Mayenfisch foundation. KKC and AG were supported by DFG SFB870 (KKC) and LMUexcellent and LMU WiFoMed (AG).

Abstract

Glycoprotein-deleted (ΔG) rabies virus-mediated monosynaptic tracing has become a standard method for neuronal circuit mapping, and is applied to virtually all parts of the rodent nervous system including the spinal cord and primary sensory neurons. Here we identified two classes of unmyelinated sensory neurons (non-peptidergic/NP- and C-LTMR/TH neurons) that are resistant to direct and transsynaptic infection from the spinal cord with rabies viruses carrying glycoproteins in their envelopes that are routinely used for infection of CNS neurons (SAD-G or N2C-G). However, the same neurons were susceptible to infection with EnvA-pseudotyped rabies virus in TVA transgenic mice, indicating that resistance to retrograde infection was due to impaired virus adsorption rather than to deficits in subsequent steps of infection. These results demonstrate an important limitation of rabies virus-based retrograde tracing of sensory neurons in adult mice, and may help to better understand the molecular machinery required for rabies virus spread in the nervous system. In this study mice of both sexes were used.

Significance Statement

In order to understand the neuronal bases of behavior it is important to identify the underlying neural circuitry. Rabies virus based monosynaptic tracing has been used to identify neuronal circuits in various parts of the nervous system. This has included connections between peripheral sensory neurons and their spinal targets, which form the first synapse in the somatosensory pathway. Here we demonstrate that two classes of unmyelinated sensory neurons, which account for more than 40% of DRG neurons, display resistance to rabies infection. Our results are therefore critical for interpreting monosynaptic rabies-based tracing in the sensory system. In addition, identification of rabies resistant neurons might provide a means for future studies addressing rabies pathobiology.

Introduction

Rabies virus infection of different parts of the nervous system has been used for more than 20 years to identify functional networks of synaptically connected neurons (Ugolini, 1995, 2008). Unequivocal identification of monosynaptically connected neurons (monosynaptic retrograde tracing) has become possible through deletion of the glycoprotein (G-protein) gene from the genome of the rabies vaccine strain SAD B19 and inclusion of fluorescent reporter genes such as GFP (Wickersham et al., 2007) for review see (Callaway and Luo, 2015; Ghanem and Conzelmann, 2016). Deletion of the G-protein coding sequence renders the virus non-infectious, while inclusion of a GFP expression cassette allows fast identification of infected neurons. Infectivity of the G-deleted rabies virus can be restored in vivo through trans-complementation of the virus with a G-protein expressed either from a plasmid, a helper virus or a mouse transgene. This complementation enables monosynaptic retrograde spread and neurons providing direct synaptic input to the primary infected cells can then be identified by the expression of the reporter gene. This powerful approach has been rapidly adapted and is now widely used for circuit mapping throughout the nervous system (for review see (Callaway and Luo, 2015)).

We and others have used this approach to identify sensory neuron subtypes providing input to defined types of second order neurons in the spinal dorsal horn. The cell bodies of these sensory neurons are located in the dorsal root ganglia (DRG) from where they send axons to the periphery and to the spinal dorsal horn. Their peripheral terminals function as detectors of mechanical, thermal, proprioceptive and noxious stimuli, while the central (spinal) terminals of these neurons form synaptic contacts with second order neurons. A comprehensive characterization of the connections between DRG neurons and spinal neurons is crucial for our understanding of how different sensory modalities are processed, modified and finally relayed to supraspinal sites where they are perceived.

Primary sensory nerve fibers can be subdivided broadly into myelinated (Aβ and Aδ) fibers and unmyelinated C-fibers. Myelinated Aβ fibers terminate predominantly in the deep dorsal horn (lamina III and deeper), while the terminals of unmyelinated C-fibers are found almost exclusively in laminae I and II. To identify the connections formed between sensory neurons and genetically defined spinal neuron populations, several groups have employed monosynaptic rabies virus-based tracing methods (Bourane et al., 2015b; Bourane et al., 2015a; Foster et al., 2015; Francois et al., 2017; Sun et al., 2017). These reports provide strong evidence for direct synaptic input from myelinated sensory fibers. However, only one study has reported retrograde infection of unmyelinated non-peptidergic (equivalent to the isolectin B4 [IB4] binding population of sensory neurons) or unmyelinated low threshold mechanoreceptive (c-LTMR / TH+) sensory neurons. This is highly unexpected as IB4+ neurons account for about 30% and TH+ for about 14% of all sensory neurons innervating the lumbar spinal dorsal horn.

To systematically investigate the ability of G-deleted rabies virus to infect all classes of DRG neurons, we directly injected G-deleted rabies virus pseudotyped with SAD-G or N2C-G rabies glycoprotein into the spinal cord of wild-type mice and determined the identity of infected DRG neurons. Using a comprehensive set of markers we found that TH+ C-LTMRs and unmyelinated non-peptidergic DRG were rarely infected. When initiating transsynaptic tracing with SAD-G complemented rabies virus from GRP-expressing spinal neurons, which are likely to receive C-LTMR and unmyelinated non-peptidergic input, we found little infection of these subclasses of DRG neurons, suggesting that they

display resistance to rabies mediated retrograde infection. Using a recently developed optimized rabies G protein (oG), slightly increased the number of non-peptidergic neurons that were infected, whereas almost no infection of TH neurons could be observed. Our results indicate that rabies-mediated tracing is biased towards myelinated neurons and is restricted from subsets of unmyelinated sensory neurons.

Material and Methods

Mice

6-8 weeks old CB57BL/6 mice of either sex were used for the injections of SAD-G and N2C-G pseudotyped G –deleted rabies. Injections of SAD-G pseudotyped G –deleted rabies were repeated in 129SVJ mice of either sex. SNS::Cre mice (Agarwal et al., 2004) and Grp::Cre mice (Gong et al., 2007) were crossed with Rosa26$^{lsl\text{-}TVA}$ (Seidler et al., 2008) to enable infection with EnvA pseudotyped rabies. SNS::Cre mice were also crossed with Rosa26$^{lsl\text{-}tdTomato}$ mice (Ai14).

Immunohistochemistry and image analysis

Mice were perfused with 4% paraformaldehyde (PFA) in PBS followed by postfixation in 4% PFA in PBS for 2 hours. DRGs were cut into 16 µm and spinal cords into 35 µm cryosections, which were mounted onto Superfrost Plus microscope slides (Thermo Scientific, Zurich, Switzerland). All primary antibodies used in this study are listed in the resource table. Secondary cyanine 3 (Cy3)-, Alexa Fluor 488-, DyLight 488-, 647- and 649-conjugated donkey antibodies were obtained from Dianova, (Hamburg, Germany). To detect IB4+ neurons the isolectin IB4 Alexa Fluor 647 conjugate (Thermo scientific) was used. Image analysis Fluorescent images were acquired on a Zeiss LSM710 Pascal confocal microscope using a 0.8 NA × 20 Plan-apochromat objective or a 1.4 NA × 40 EC Plan-Neofluar oil-immersion objective and the ZEN2012 software (Carl Zeiss). Whenever applicable, contrast, illumination, and false colors were adjusted in ImageJ or Adobe Photoshop (Adobe Systems, Dublin, Ireland). The number of immunoreactive cells was determined in 10µm z-stacks using the ImageJ Cell Counter plug-in.

Rabies virus preparation and terminology

All rabies viruses used in this study were derived from the SAD ΔG rabies in which the G-gene was replaced by either eGFP or mCherry (SAD.RabiesΔG.eGFP/mCherry). SAD.RabiesΔG.XFP viruses were pseudotyped with SAD-G, N2C-G or EnvA glycoproteins resulting in SAD.RabiesΔG.XFP (SAD-G), SAD.RabiesΔG.XFP (N2C-G) or SAD.RabiesΔG.XFP (EnvA) respectively. Pseudotyped SAD ΔG rabies virus was generated as described in Foster et al., (2015) and complemented as described previously (Wickersham et al., 2007). SAD.RabiesΔG.mCherry (N2c-G) was generated by transfecting HEK293T cells with pMD.RVG.CVS24-N2c (addgene #19712, deposited by Manfred Schubert) and infecting the transfected cells with SAD.RabiesΔG.mCherry (SAD-G) (MOI=0.01) Supernatants were harvested and concentrated as described previously (Wickersham et al., 2007).

AAV preparation

AAV.flex.mCherry-2A-RabG vector was cloned in-house and packaged at Penn Vector Core (Perelman School of Medicine, University of Pennsylvania) using their custom service. AAV.flex.mCherry-2A-RabG vector was cloned by excising the ChR2-mCherry fusion protein from pAAV-Ef1a-DIO-hChR2(H134R)-mCherryWPRE-pA (kindly provided by Dr. Karl Deisseroth, Stanford University) with

AscI and NheI and replacing it with PCR amplified mCherry-2A-RabG cDNA. pAAV-Ef1a-DIO-oG-WPRE-hGH was obtained from Addgene (74290 / (Kim et al., 2016)) and packaged by the Viral Vector Facility (Zurich). AAV 2/1 vectors were used in this study.

Intraspinal virus injections

Mice between 6-8 weeks old were anesthetized with 2 - 5% isofluorane and lumbar vertebrae L4 and L5 were exposed. The animal was then placed in a motorized stereotaxic frame and the vertebral column was immobilized using a pair of spinal adaptors. The vertebral lamina and dorsal spinous process were removed to expose the L4 lumbar segment. The dura was perforated about 500 µm to the left of the dorsal blood vessel using a beveled 30G needle. Viral vectors were injected at a depth of 200 - 300 µm using a glass micropipette (tip diameter 30 - 40 µm) attached to a 10 µl Hamilton syringe. The rate of injection (30 nl/min) was controlled using a PHD Ultra syringe pump with a nanomite attachment (Harvard Apparatus, Holliston, MA). The micropipette was left in place for 5 min after the injection. In all experiments where rabies virus was injected two individual injections at 500nl each spaced approximately 1 mm apart were made. Wounds were sutured and the animals were injected i.p. with 0.03 mg/kg buprenorphine and allowed to recover on a heat mat. Rabies virus injected mice were perfusion fixed 3-10d after injection.

Retrograde tracing experiments

For retrograde monosynaptic tracing experiments, we used a two-step strategy that involved injection an AAV helper virus (AAV.flex.mCherry-2A-SAD-G or AAV.Ef1a.DIO.oG.WPRE.hGH) containing either a Cre-dependent mCherry and rabies glycoprotein (SAD-G) expression cassette or the cDNA of optimized rabies glycoprotein (oG) followed by a subsequent injection of an EnvA (avian sarcoma leukosis virus “A” envelop glycoprotein) pseudotyped glycoprotein-deficient rabies virus (SAD.RabiesΔG.eGFP (EnvA)). The TVA protein expressed from the Rosa26 reporter mouse line enabled cell type specific infection of Grp::Cre+ neurons, and the SAD-G or oG was expressed to transcomplement the glycoprotein-deficient rabies virus in the primary infected neurons. Grp::Cre+ mice received two unilateral injections of AAV.flex.mCherry-2A-RabG / AAV.Ef1a.DIO.oG.WPRE.hGH (2.9×10^9 GC per injection in 300 nl) into L3 and L4 segments of the dorsal horn. The vertebral lamina was left intact in order to limit the adhesion of scar tissue to the dorsal surface of the spinal cord. The mice were allowed to recover and then 14 days after they received an injection of SAD.RabiesΔG.eGFP (EnvA) (1×10^6 GC per injection in 500 nl) into the same site. Spinal cord and DRGs were harvested 5 days later.

Formalin injections

For evaluation of the activity dependency of rabies infection, 10µl of 5% formalin (Paraformaldehyde Granular; Electron Microscopy Science) dissolved in PBS was injected subcutaneously into the left hindpaw of the mouse immediately after the spinal injection of SAD.RabiesΔG.eGFP (SAD-G) virus. The mouse was kept under isoflurane anesthesia for 1h following formalin injection. Buprenorphine (Tamgesic; 3µg per mouse, subcutaneously) was given post-operatively before the mouse recovered from anesthesia.

Resource table

Reagent	**resource**	**identifier**

Antibodies (dilution)		
647-IB4 (1:500)	Thermo scientific	I32450
rabbit anti-CGRP (1:1000)	Immunostar	RRID:AB_572217
chicken anti-GFP (1:1000)	LifeTechnologies	RRID:AB_2534023
rabbit anti-GFP (1:1000)	Molecular Probes	RRID:AB_221570
Rabbit anti-Homer1 (1:500)	SynapticSystems	RRID:AB_2120990
guinea pig anti-Lmx1b (1:10 000)	Dr Carmen Birchmeier	(Muller et al., 2002)
rat anti-mCherry (1:1000)	Molecular Probes	RRID:AB_2536611
rabbit anti-NF200 (1:1000)	Sigma	RRID:AB_477272
rabbit anti-NeuN (1:1000)	Abcam	RRID:AB_10711153
rabbit anti P2X3 (1:1000)	Abcam	RRID:AB_297006
sheep anti-PlxnC1 (1:400)	R&D Systems	RRID:AB_2284038
sheep anti-TH (1:1000)	Millipore	RRID:AB_90755
goat anti-TrkA (1:400)	R&D Systems	RRID:AB_2283049
Viruses		
AAV1.EF1a.flex.mCherry-2A-SADG	Penn Vector Core (Philadelphia, US)	Custom production
pAAV1.Ef1a.DIO.oG.WPRE.hGH	Viral Vector Facility (Zurich)	Custom production
SAD.RabiesΔG.eGFP (EnvA)	Produced for this publication	
SAD.RabiesΔG.mCherry (SAD-G)	Produced for this publication	
SAD.RabiesΔG.eGFP (SAD-G)	Produced for this publication / GENE TRANSFER, TARGETING AND THERAPEUTICS CORE (Salk Institute)	
SAD.RabiesΔG.mCherry (N2C-G)	Produced for this publication	
Mice		
C57BL/6J	Institute of Pharmacology (Zurich)	RRID:IMSR_JAX:000664
129SVJ	Institute of Pharmacology (Zurich)	RRID:IMSR_JAX:000691
Grp::Cre	MMRRC	RRID:MMRRC_037585-UCD
Rosa26$^{lsl\text{-}TVA}$	Dieter Saur	(Seidler et al., 2008)
Rosa26$^{lsl\text{-}tdTomato}$	The Jackson Laboratory	RRID:IMSR_JAX:007908
Sns::Cre	Rohini Kuner	(Agarwal et al., 2004)
Plasmids		
pAAV-Ef1a-DIO-oG-WPRE-hGH	Addgene (RRID:SCR_002037)	74290
pMD.RVG.CVS24-N2c	Addgene(RRID:SCR_002037)	19712

176

177 Gene enrichment and pathway analysis

178 To compare gene expression profiles of TH and PEP2,NF1,NF2 populations, we downloaded the
179 external resource table 2 from Usoskin et al (http://linnarssonlab.org/drg/ (External resource Table
180 2). In Excel we applied the following two filter combinations: 1. less than or equal to 0.05 for the TH

column & greater than or equal to 0.2 for the PEP2, NF2 and NF3 columns. 2. Less than or equal to 0.01 for the NF2, NF3 and PEP2 columns & greater than or equal to 0.2 for the TH column.
The resulting gene lists were subjected to a pathway analysis using GSEA (gene set enrichment analysis, GSEA software, and Molecular Signature Database (MSigDB) (Subramanian, Tamayo, et al. (2005), PNAS 102, 15545-15550, http://www.broad.mit.edu/gsea/).

Experimental design

For each experimental set the respective pseudotyped rabies variant was injected into the dorsal horn of 4-8 mice. For all cell counts, sections were prepared from 4-8 animals and at least four sections were analyzed per animal. In order to avoid the double counting of cells in adjacent sections, all sections used for quantification were taken at least 50 µm apart. To determine the prevalence of neurons in lumbar DRGs of CB57BL/6 wildtype mice 6162 cells were evaluated. For the characterization of DRG neurons that became infected by spinal injection of SAD-G or N2C-G, 1059 and 1223 eGFP+ cells were analyzed, respectively. In order to determine the effect of neuronal activity on rabies transduction 649 eGFP+ cells were analyzed. For the characterization of recombination positive cells in SNS::Cre; Rosa26$^{lsl\text{-}tdTomato}$ mice 4820 cells were analyzed. To evaluate the ability of Enva-pseudotyped G-deleted rabies to transduce TVA-expressing SNS neurons 124 eGFP+ cells were analyzed. To determine the efficiency of transsynaptic tracing initiated from spinal Grp+ neurons 202 (SAD-G complemented rabies) and 599 (oG complemented rabies) eGFP+ cells were analyzed.

Statistics

Microsoft excel was used for statistical analysis. A two-way paired t-test was used for the analysis of activity dependent infection efficiencies.

Results

Prevalence of neuronal subsets in lumbar wild-type DRGs

In order to understand whether rabies-mediated retrograde tracing allows infection of all sensory neuron populations we analyzed their susceptibility to rabies virus infection in a systematic and comprehensive manner. We first evaluated suitable molecular markers for the identification of the different subclasses of DRG neurons that have recently been proposed (Usoskin et al., 2015). Based on single cell RNA sequencing this study suggested four major classes of DRG neurons; NF neurons (neurofilament positive DRG neurons including all low threshold mechanorecpetors [LTMRs] and proprioceptors), NP neurons (nonpeptidergic DRG neurons with unmyelinated axons), peptidergic (PEP) neurons, (subdivided into unmyelinated PEP1 neurons and myelinated PEP2 neurons) and tyrosine hydroxylase (TH) expressing neurons (unmyelinated C-fiber LTMRs). We compared molecular markers established by Usoskin et al. 2015 to the widely used IB4 labeling and CGRP (calcitonin gene-related peptide) antibody staining. We found that the IB4 binding population of sensory neurons largely overlaps with the Plxnc1;P2X3 double-positive population and that the TrkA+ and CGRP+ sensory neuron populations were virtually identical (Fig. 1C,D). A small fraction of Plxnc1;P2X3 double-labeled neurons did not bind IB4 and vice versa. When analyzing the fraction of

NF200+ neurons we found, as previously reported by others, that NF200+ neurons can be subdivided into NF200+,CGRP+ and NF200+,CGRP- neurons (Fig. 1A) and that the binding of IB4 and expression of TH are mutually exclusive (Fig. 1B). These findings are consistent with the results obtained by Usoskin at al.2015. We therefore chose the following antibodies and antibody combinations for sensory neuron classification; anti-NF200 antibody (NF and PEP2 neurons), co-labeling with antibodies against Plxnc1 and P2X3 (NP neurons), antibodies against TrkA (PEP and NP2 neurons) and anti-TH antibodies (TH neurons/C-LTMRs) (Fig 1F). We then quantified the fraction of neurons labeled with these markers against the number of NeuN+ neurons in lumbar L3/L4/L5 DRGs of C57BL/6 wild-type mice. We found that 45.5 ± 8.5% of DRG neurons were NF200+ (corresponding to NF plus PEP2 neurons), 32.0 ± 7.7% were Plxnc1+;P2X3+ (NP neurons), 29.3 ± 8.7% were TrkA+ (NP2 and PEP) and 13.6 ± 5.4% were TH+ (TH neurons) (Fig 1 E and F). These data are in agreement with previously determined percentages of DRG neuron subtypes (McCoy et al., 2013).

Injected SAD-G or N2C-G pseudotyped G-deleted rabies virus fails to infect NP and TH neurons

SAD-G rabies glycoprotein has been used for trans-complementation in most monosynaptic retrograde tracing studies. To determine whether rabies-G coated modified rabies can equally infect the central terminals of primary afferents of all classes of DRG neurons we injected SAD.RabiesΔG-mCherry (SAD-G) or SAD.RabiesΔG-eGFP (SAD-G) into the spinal cord of C57BL/6 wild-type mice. We first determined an optimal incubation time for our analysis. A longer incubation time will lead to increased fluorescence due to an accumulation of the rabies encoded marker gene product, but infection with modified rabies is cytotoxic after a certain incubation time (Wickersham et al., 2007; Reardon et al., 2016). In our hands, DRG neurons are sensitive to rabies infection and start to downregulate endogenous proteins such as NeuN at 7-8d post infection. However, other groups have found maximum infection efficiency after 10d in different parts of the nervous system (Wertz et al., 2015). We therefore analyzed infection of DRG neurons at 5d and 10d following intraspinal injection of rabies virus. Five days after intraspinal injection of SAD.RabiesΔG-mCherry (SAD-G) all infected DRG neurons expressed NeuN (Fig 2 A). In contrast, at 10d after injection we rarely found any mCherry+ DRG cell bodies, although mCherry+ axons were still detectable (Fig 2 B). In addition, we observed a strong increase in macrophage infiltration evident by the upregulation of IBA1 at 10d as compared to 5d post injection (Fig 2 C+D). This suggests that prolonged expression and replication of the SAD.RabiesΔG-mCherry genome rapidly becomes cytotoxic for DRG neurons. We therefore performed subsequent experiments at 5d post injection.

Five days after injection of SAD.RabiesΔG-mCherry/eGFP (SAD-G) into the left lumbar dorsal horn, numerous neuronal cell bodies throughout laminae I-IV became positive for the respective fluorescent marker (Fig 3A+B) suggesting that the primary afferent terminals of this area were also exposed to the rabies virus. We then analyzed the molecular profile of SAD.RabiesΔG-mCherry infected (mCherry+) DRG neurons and found that 91.3±9.7% were NF200+ (NF plus PEP2 neurons), 1±2% were Plxnc1+;P2X3+ (NP), 66.2±17.5% were TrkA+ (NP2, PEP) and 0.2±1% were TH+ (TH) (Fig. 3C-F). Compared to the prevalence of neurons labeled with each respective marker in wild-type DRGs (Fig. 1E), Plxnc1+;P2X3+ and TH+ labeled neurons were under-represented whereas NF200+ and TrkA+ labeled neurons were over-represented. Almost identical results were obtained when using SAD.RabiesΔG-eGFP (SAD-G) or a different genetic background of mice (129SvJ).

To exclude the possibility that the inability of SAD.RabiesΔG-mCherry (SAD-G) to infect NP or TH neurons was specific to the SAD-G protein derived from an attenuated vaccine strain we repeated

these experiments with SAD.RabiesΔG-mCherry (N2C-G), which was pseudotyped with the G protein of the challenge virus strain (CVS) variant N2C (N2C-G) (Fig. 3A). This strain has been reported to have a higher neurotropism (Morimoto et al., 1998; Reardon et al., 2016). Like in the previous experiment we observed neuronal loss at 10d but not at 5d after injection of SAD.RabiesΔG-mCherry (N2C-G) (data not shown). When we determined the neuronal identity 5d after injection, we obtained very similar results as after injection of SAD.RabiesΔG-mCherry (SAD-G). Of the mCherry labeled DRG neurons 97±2.6% were NF200+, 1±2.2% Plxnc1+;P2X3+, 58±18.8% TrkA+ and 0.7±2.1% TH+ (Fig. 3 G-J) indicating that the central terminals of NP and TH neurons are largely resistant to retrograde infection with either SAD-G or N2C-G pseudotyped rabies virus.

We next addressed whether the bias towards infection of myelinated sensory neurons was due to different activity levels of sensory neuron subtypes during exposure to the rabies virus. In unchallenged mice, myelinated touch-sensitive neurons and proprioceptive neurons likely exhibit higher levels of activity than unmyelinated nociceptors and pruritoceptors. To test whether neuronal activity increases rabies virus infection we injected the rabies virus into the spinal cords of mice under conditions that tonically activate nociceptors. We injected the TRPA1 agonist formalin (McNamara et al., 2007) subcutaneously into the hind paw of mice immediately after spinal injection of SAD.RabiesΔG-eGFP (SAD-G) (Fig. 4A). Subcutaneous injection of formalin induces tonic activity in nociceptive nerve fibers that innervate the injected skin area (Fischer et al., 2015). The IB4+ subpopulation of unmyelinated sensory neurons (equivalent to NP neurons), most of which function as nociceptors or pruritoceptors, is highly susceptible to formalin excitation as expression of TRPA1 channels is particularly strong in these neurons (Barabas et al., 2012). When comparing the infection rate of sensory neurons between naïve mice and formalin-treated mice, we found that there was indeed a significant increase in the percentage of labeled DRG neurons in the formalin injected group (5.0 ± 2.1% in formalin injected mice versus 1.6 ± 1.2% of labeled neurons in naïve mice, t-test $p = 0.007$) (Fig. 4B). However, despite this formalin-induced increase in the total number of infected DRG neurons, we still did not find infected NP or TH neurons (Fig. 4C-F). The resistance of these neurons to infection by SAD.RabiesΔG-eGFP (SAD-G) is hence unrelated to low neuronal activity during virus exposure.

NP neurons can support virus replication and expression of viral genes

We then tested whether the absence of efficient labeling of TH or NP neurons was due to the inability of rabies G-coated SAD.RabiesΔG-eGFP to enter these neurons or whether it was due to a deficiency in some post-infection processes. These could include the axonal transport of the SAD.RabiesΔG-eGFP, viral transcription and replication or translation of the proteins encoded by the rabies virus genome. To this end, we generated sns::Cre; $Rosa26^{lsl\text{-}TVA}$ double transgenic mice, in which the Cre-recombinase is expressed in all unmyelinated sensory neurons (Agarwal et al., 2004). We then injected the lumbar spinal cord of these double transgenic mice with EnvA pseudotyped SAD.RabiesΔG-eGFP. This strategy bypasses the typical pathway of virus entry and direct infection of unmyelinated fibers via the interaction of the EnvA G-protein with the TVA receptor. To verify that NP and TH neurons of sns::Cre; $Rosa26^{lsl\text{-}TVA}$ mice expressed the TVA receptor, we first characterized the recombination pattern mediated by the sns::Cre driver in sns::Cre; $Rosa26^{lsl\text{-}Tomato}$ mice. In these mice, Plxnc1+;P2X3+, TrkA+, and all TH+ neurons expressed Tomato indicating that also Cre was expressed in all NP, PEP and TH neurons (Fig 5 A-C). In the spinal cord strong Tomato+ central axons were seen in LI+II but weaker expression was also observed in LIII and IV (Fig. 5D). As expected, Tomato-negative DRG neurons were NF200+ but TrkA negative and thus belonged to the NF

population of non-nociceptive somatosensory and proprioceptive neurons (Fig. 5C). Conversely, we found that 54.5% of Tomato+ neurons were Plxnc1+;P2X3+, 46.3% were TrkA+ and 14.6% were TH+ (Fig. 5E). We then injected SAD.RabiesΔG-eGFP (EnvA) into the spinal cord of sns::Cre; Rosa26$^{lsl\text{-}TVA}$ mice (Fig. 6A) and characterized the markers expressed by the eGFP+ DRG neurons. 59% of the eGFP+ neurons expressed NF200, 38% co-expressed Plxnc1 and P2X3, and 68% expressed TrkA but we found no co-expression with TH (Fig. 6B-E). Expression of eGFP in Plxnc1+;P2X3+ neurons indicated that NP neurons possess the machinery to support virus replication and the expression of proteins encoded by the rabies virus genome. It is therefore likely that the failure to infect the central terminals of NP neurons underlies the resistance of NP DRG neurons to SAD-G/N2C-G coated-rabies-mediated infection.

TH and NP neurons are resistant to transsynaptic tracing with SAD-G pseudotyped rabies, but display low susceptibility to transsynaptic tracing with oG pseudotyped rabies

Ruigrok et al. (2016) recently suggested that infection via the extracellular space and transneuronal/transsynaptic infection might rely on different mechanisms. In order to test whether NP and TH neurons are equally resistant to either transneuronal or direct spinal infection by G-complemented rabies, we investigated a spinal subpopulation that should receive input from NP and TH neurons.

Spinal Grp+ neurons are second order excitatory neurons located in an area of the superficial dorsal horn, that overlaps with the termination zone of NP and TH neurons (LIIi and LIIiv respectively). In sections obtained from Grp::Cre; Rosa26$^{lsl\text{-}Tom}$ mice, a profound regional overlap of tdTomato with CGRP+ (PEP + NP2), IB4+ (NP) and vGlut3+ (TH) immunofluorescence was observed (Fig 7A). To provide further evidence for direct synaptic contacts between Grp neurons and IB4+ and/or vGlut3+ primary sensory axon terminals, we used IB4/vGlut3 labeling in combination with an antibody against the postsynaptic marker protein Homer1 on Grp::Cre; Rosa26$^{lsl\text{-}Tom}$ mice (Gutierrez-Mecinas et al., 2016). We found IB4+ and vGlut3+ terminals directly opposing Homer1 labeled postsynapses on Grp neurons (Fig 7B+C).

To initiate retrograde tracing from Grp+ spinal neurons, Grp::Cre mice were crossed with TVA reporter mice (Rosa26$^{lsl\text{-}Tva}$). Double transgenic mice derived from these breedings were injected with an AAV.flex.mCherryT2A-SAD.G helper virus into the left lumbar spinal cord to allow complementation of the G-deleted rabies in Cre+ neurons. Two weeks later, we injected pseudotyped SAD.RabiesΔG-eGFP (EnvA) into the same site. Five days after rabies virus injection we observed numerous eGFP+ neurons in the spinal cord. Many of these were mCherry negative suggesting successful secondary (retrograde) infection (Fig 7D). We also detected numerous eGFP+ neurons in the DRGs of these injected mice (Fig 7E). None of the DRG neurons were mCherry positive verifying that these neurons were secondary infected cells. We then analyzed the molecular profile of the retrogradely infected DRG neurons. Using the same set of antibodies as before, we found that nearly all infected neurons (97%±2.7) were NF200+. About half of these neurons, also expressed TrkA (47.8%±12.1), but none of the infected neurons were found to be NP or TH neurons (Fig 7F).

Recently an optimized rabies G protein (oG) has been developed to allow for more efficient transsynaptic tracing (Kim et al., 2016). We therefore repeated the transsynaptic tracing experiment and injected an AAV.flex.oG helper virus into the spinal cord of Grp::Cre; Rosa26$^{lsl\text{-}Tva}$. Indeed, when analyzing the identity of infected DRG neurons we found a shift in the molecular profile. Using the oG rabies G-protein led to a relative increase in infected TrkA+ versus NF200+ DRG neurons. In these

experiments a small number of infected NP (7.2±2%) and TH neurons (1.2±0.7%) was also apparent (Fig 7F). However, given the abundance of TH and IB4 terminals forming synaptic contacts with Grp neurons, the number of infected NP, and TH neurons in particular, was much lower than expected. This indicated a high degree of resistance of TH and IB4 neurons to rabies virus infection, including those pseudotyped with the oG-glycoprotein.

TH neurons show differences in expression of membrane proteins compared to DRG subpopulation that are highly susceptible to rabies infection

We have identified DRG neurons of the TH class as being largely resistant to SAD ΔG rabies virus pseudotyped with three different variants of rabies glycoprotein. We reasoned that the resistance to rabies infection displayed by TH neurons could either be due to the lack of proteins that are required for rabies uptake, transport or unloading and translation of the rabies genome or to the presence of proteins that prevent any of these steps. To obtain first insights into the potential mechanisms conferring resistance to TH neurons we analyzed whole transcriptome data provided by Usoskin and colleagues (http://linnarssonlab.org/drg/ (External resource Table 2). First, we analyzed this data for the expression of three protein families that have been described as potential rabies receptors. These included the nicotinic acetylcholine receptor (nAChR), neural cell adhesion molecule (NCAM) and the low affinity neurotrophin receptor (p75NTR/ Ngfr) (Lentz et al., 1983; Thoulouze et al., 1998; Tuffereau et al., 1998a; Tuffereau et al., 1998b; Langevin and Tuffereau, 2002). NCAM1/2 and p75NTR (Ngfr) were expressed in a similar or even higher proportion of TH cells when compared with the NF and PEP2 subclasses which were susceptible to rabies infection (Table 1). Also among the different nAChR subunits we could not identify any that were expressed in NF and PEP2 neurons but absent from in TH neurons (Table 1). In our analysis we found rabies infected NF200+ DRG neurons that belonged to the PEP2 (NF200+, TrkA+) and NF2/3 subgroups (NF200+, Calb1+ or NF200+, TrkC+ data not shown / markers for NF1 or NF4/5 were not analyzed). We next performed a genome wide analysis and exploited again the transcriptomics data from Usoskin et al. and searched for genes that were either enriched or depleted in TH neurons. To this end, we applied two criteria. First, we filtered for genes that were detected in at least 20% of the susceptible subpopulations but in less than 5% of the TH class. Second, we identified all genes that were detected in at least 20% of the TH population but in less than 10% of NF2/3 and PEP populations. We identified 321 genes that were not expressed in TH neurons and 52 genes that were detected in more than 20% of TH neurons but not in PEP2 and NF2/3 neurons (extended Data Table 1 and 2). GO-term pathway analysis (GSEA) of the list of genes lacking in TH neurons revealed that the functions of the differentially expressed genes relate to “NEURON PART SYNAPSE”, “NEURON PROJECTION”, “REGULATION OF ANATOMICAL STRUCTURE MORPHOGENESIS” and “REGULATION OF TRANSPORT”. These results suggest that resistant TH neurons and sensitive PEP2 and NF2/3 neurons differ significantly in synapse function or morphology. As wild-type rabies virus spreads in the CNS via synapses, it is tempting to speculate that some of these genes are involved in neuronal infection by rabies virus

Discussion

Here we have shown that two classes of unmyelinated sensory neurons (NP and TH neurons), which account for almost half of the total DRG neuron population, are largely resistant to rabies virus infection from the spinal cord (Fig. 8). These findings have important implications for the interpretation of studies using transsynaptic rabies virus-based tracing of sensory neurons.

Limitations of rabies mediated circuit tracing

Unmyelinated NP and TH sensory nerve fibers serve several important functions in somatosensation. The NP subgroup corresponds mainly to non-peptidergic unmyelinated fibers that bind IB4 and primarily innervate the skin. In rodents, their activation provokes withdrawal responses or scratching behavior. It is therefore generally accepted that activation of these fibers elicits pain and itch sensations (Basbaum et al., 2009; Braz et al., 2014). TH is a marker for very particular C type sensory fibers that also innervate the skin, but are activated by low intensity mechanical stimuli. These fibers are called C-type low threshold mechanoreceptors (Zotterman, 1939; Li et al., 2011). It is believed that their activation elicits pleasant sensations (Olausson et al., 2010). All of these fiber types terminate either in the superficial layers of the spinal dorsal horn (for those originating in the body trunk and extremities) or in the trigeminal nucleus (in the case of fibers innervating the head). Understanding how these different fibers interact with different types of central neurons is critical to understand how different sensory modalities are processed. The synaptic contacts underlying these innervation patterns are in most studies assessed with retrograde rabies virus based tracing experiments. Our results are in agreement with several studies that also failed to identify significant input to various dorsal horn neuron populations from NP (IB4+ or P2X3+/Plxnc1+) or TH (TH+) neurons (Bourane et al., 2015b; Bourane et al., 2015a; Foster et al., 2015; Francois et al., 2017). These are unexpected findings, particularly for those dorsal horn neuron populations that are present in lamina II (Npy+ and Penk+), the termination zone of NP and TH neurons. This finding also contrasts with electrophysiological evidence showing that all morphological classes of Lamina II neurons receive input from NP neurons (MrgrpD+ neurons (Wang and Zylka, 2009)). One potential reason for the observed resistance to rabies infection could have been neuronal inactivity. Anecdotal clinical results (Willoughby et al., 2005) and unpublished results in the rabies community have suggested that the activity status of neurons might have an impact on infectivity by rabies virus. By injecting formalin immedeatly after injection of SAD-G pseudotyped SAD.rabiesΔG-eGFP we stimulated the activity of NP neurons at the time point of infection. Yet, we did not see an increase in the percentage of infected NP neurons. Nevertheless, we detected a significant increase in the overall percentage of infected neurons. Secondary effects of formalin injections are pro-inflammatory responses which might alter NF and PEP neurons in a way that increase their susceptibility to rabies infection. In conclusion, we have demonstrated that negative results in retrograde tracing experiments need to be interpreted with greater caution, and additional techniques need to be used to verify the absence of synaptic innervation.

In a recent study addressing the function of spinal Grp neurons, rabies tracing has also been used to identify input to Grp+ spinal interneurons (Sun et al., 2017). Although in this study and in ours the same Grp::Cre transgenic mice have been used, both studies yielded markedly different results. Both studies found more than 50% of the labelled DRG neurons to be CGRP+/TrkA+. However, while we could not detect any labelling of NP neurons (PlxnC1+; P2X3+) when using SAD-G pseudotyped rabies Sun et al., (2017) found that more than 30% of the labelled DRG neurons were of the NP (IB4+) subtype. These differences are difficult to explain, but differences in age, a previous injury to DRG neurons, or a slightly longer incubation time may provide explanations. A higher susceptibility of NP neurons at early postnatal stages has been suggested by Zhang et al. (2015), who showed that peripheral nociceptors (NP+PEP neurons) can be efficiently infected at P3 (Zhang et al., 2015). Alternatively, a nerve injury that is potentially caused by the preceding injection of the helper virus (coding for TVA and SAD-G) could result in more neurons being labeled. Solorzano et al. (2015) have indeed demonstrated that Grp is upregulated in DRG neurons upon nerve injury (Solorzano et al.,

2015). If nerves were injured during the first injection, TVA may have been expressed in DRG neurons, including neurons of the NP subtype. These neurons would then have been susceptible to direct infection by the EnvA pseudotyped rabies. Finally, Sun et al. have used a 7d incubation time, which was 2d more than the incubation time we have chosen for this study. This might allow for the detection of neurons with low levels of retrograde infection.

As previously reported we also found that DRG neurons were sensitive to infection with the fixed rabies virus strain SAD (Reardon et al., 2016). Prolonged replication and expression of the SAD.RabiesΔG-XFP (≥10d) led to neurotoxicity and almost complete loss of infected neurons, regardless of whether the modified rabies was pseudotyped with the SAD-G or the N2C-G glycoprotein. It thus seems as though the rapid amplification and expression of the SAD.RabiesΔG-XFP genome is responsible for neurotoxicity. Retrograde tracing experiments using the SAD.RabiesΔG strain in the peripheral nervous system should therefore be limited to ≤7d post infection.

Implications for understanding the pathobiology of rabies virus

In the past few decades significant progress has been made in understanding rabies pathogenesis, for example by identifying host proteins that can mediate rabies infection (for review see (Sissoeff et al., 2005; Albertini et al., 2012)). Yet, none of the identified proteins are essential for rabies virus infection. Indeed, our analysis of transcriptomic data available from the Linnarsson and Ernfors labs (http://linnarssonlab.org/drg/(Usoskin et al., 2015)) showed that none of the expression patterns of the identified rabies receptors (nAChR, NCAM or p75NTR/ Ngfr) could explain the resistance of TH (NP) neurons to rabies infection. Nevertheless, by comparing the transcriptomes of DRG subpopulations susceptible to rabies infection with the transcriptome of the TH population we identified 321 genes that were lacking in the TH population and 57 that were enriched in the TH population. Pathway analysis of the genes lacking in the TH population indicated significant morphological and structural differences of TH compared to rabies susceptible DRG neurons. Interestingly, we recently reported that retrograde (axonal) transduction of DRG neurons by adeno-associated viruses (AAV) also displayed a bias for transduction of NF200+ neurons and against TH and IB4 neurons (Haenraets et al., 2017). It is therefore conceivable that some morphological/structural properties of NP and TH neurons or their central axons impair virus uptake. This might either be due to genes that are selectively expressed in these populations or absent from them. Future detailed functional analysis of e.g. surface proteins that are differentially expressed in TH neurons should therefore provide insights into the mechanisms of virus uptake and expression.

Alternative strategies for the identification of sensory input onto spinal neurons

Rabies-mediated monosynaptic tracing remains a powerful tool to identify direct input to individual neurons or genetically defined subsets of neurons, and we find that the G-deleted rabies pseudotyped with the recently developed oG-glycoprotein leads to a greater infection of connected neurons. However, our results also indicate that if rabies tracing is used to determine peripheral input in adult mice, negative results need to be interpreted with greater caution. Other retrograde tracer such as pseudorabies or Tetanus toxin C-fragment fusion proteins might be used for verification, but their ability to infect the central terminals of all DRG neuron classes must also be

verified first. When using rabies for tracing sensory input, one should complement results obtained with other methods such as electrophysiology, which has also been used to determine the type of primary afferent input (e.g. (Wang and Zylka, 2009)). In addition, anterograde tracing initiated from distinct DRG subtypes could be used to determine synaptic input from distinct DRG subtypes (Braz et al., 2005). An unbiased approach could be based on the mGRASP system where a pre-mGRASP would be expressed in DRG neurons and a Cre dependent post-mGRASP in the spinal subpopulation of interest (Kim et al., 2011). Immunohistochemical analyses at the level of GFP-labeled spinal synapses will then provide insights into the type of input that is provided by primary afferents.

Author contributions

GA performed virus injections and performed and analyzed morphological experiments. K.K.C. and A.G. produced and provided the majority of pseudotyped G-deleted rabies viruses used in this study. EF performed virus injections. HW analyzed experiments. H.W. and H.U.Z. designed experiments and wrote the manuscript. All authors have commented on the manuscript.

Acknowledgements

This work was supported by an ERC Advanced Investigator Grant (DHISP 250128) a grant from the Swiss National Research Foundation (156393) and a Wellcome Trust Collaborative Award in Science (200183/Z/15/Z) (to H.U.Z.). HW was supported by the Olga Mayenfisch foundation. KKC and AG were supported by DFG SFB870 (KKC) and LMUexcellent and LMU WiFoMed (AG). We are grateful to D. Saur for providing Rosa26^{TVA} mice and C. Birchmeier for the Lmx1b antibody. We are grateful to Robert Ganley for commenting on and correcting the manuscript.

Literature

Agarwal N, Offermanns S, Kuner R (2004) Conditional gene deletion in primary nociceptive neurons of trigeminal ganglia and dorsal root ganglia. Genesis 38:122-129.

Albertini AA, Baquero E, Ferlin A, Gaudin Y (2012) Molecular and cellular aspects of rhabdovirus entry. Viruses 4:117-139.

Barabas ME, Kossyreva EA, Stucky CL (2012) TRPA1 is functionally expressed primarily by IB4-binding, non-peptidergic mouse and rat sensory neurons. PloS one 7:e47988.

Basbaum AI, Bautista DM, Scherrer G, Julius D (2009) Cellular and molecular mechanisms of pain. Cell 139:267-284.

Bourane S, Grossmann KS, Britz O, Dalet A, Del Barrio MG, Stam FJ, Garcia-Campmany L, Koch S, Goulding M (2015a) Identification of a spinal circuit for light touch and fine motor control. Cell 160:503-515.

Bourane S, Duan B, Koch SC, Dalet A, Britz O, Garcia-Campmany L, Kim E, Cheng L, Ghosh A, Ma Q, Goulding M (2015b) Gate control of mechanical itch by a subpopulation of spinal cord interneurons. Science 350:550-554.

Braz J, Solorzano C, Wang X, Basbaum AI (2014) Transmitting pain and itch messages: a contemporary view of the spinal cord circuits that generate gate control. Neuron 82:522-536.

Braz JM, Nassar MA, Wood JN, Basbaum AI (2005) Parallel "pain" pathways arise from subpopulations of primary afferent nociceptor. Neuron 47:787-793.

Callaway EM, Luo L (2015) Monosynaptic Circuit Tracing with Glycoprotein-Deleted Rabies Viruses. J Neurosci 35:8979-8985.

Fischer MJ, Soller KJ, Sauer SK, Kalucka J, Veglia G, Reeh PW (2015) Formalin evokes calcium transients from the endoplasmatic reticulum. PloS one 10:e0123762.

Foster E, Wildner H, Tudeau L, Haueter S, Ralvenius WT, Jegen M, Johannssen H, Hosli L, Haenraets K, Ghanem A, Conzelmann KK, Bosl M, Zeilhofer HU (2015) Targeted ablation, silencing, and activation establish glycinergic dorsal horn neurons as key components of a spinal gate for pain and itch. Neuron 85:1289-1304.

Francois A, Low SA, Sypek EI, Christensen AJ, Sotoudeh C, Beier KT, Ramakrishnan C, Ritola KD, Sharif-Naeini R, Deisseroth K, Delp SL, Malenka RC, Luo L, Hantman AW, Scherrer G (2017) A Brainstem-Spinal Cord Inhibitory Circuit for Mechanical Pain Modulation by GABA and Enkephalins. Neuron 93:822-839 e826.

Ghanem A, Conzelmann KK (2016) G gene-deficient single-round rabies viruses for neuronal circuit analysis. Virus research 216:41-54.

Gong S, Doughty M, Harbaugh CR, Cummins A, Hatten ME, Heintz N, Gerfen CR (2007) Targeting Cre recombinase to specific neuron populations with bacterial artificial chromosome constructs. J Neurosci 27:9817-9823.

Gutierrez-Mecinas M, Kuehn ED, Abraira VE, Polgar E, Watanabe M, Todd AJ (2016) Immunostaining for Homer reveals the majority of excitatory synapses in laminae I-III of the mouse spinal dorsal horn. Neuroscience 329:171-181.

Haenraets K, Foster E, Johannssen H, Kandra V, Frezel N, Steffen T, Jaramillo V, Paterna JC, Zeilhofer HU, Wildner H (2017) Spinal nociceptive circuit analysis with recombinant adeno associated viruses: the impact of serotypes and promoters. Journal of neurochemistry.

Kim EJ, Jacobs MW, Ito-Cole T, Callaway EM (2016) Improved Monosynaptic Neural Circuit Tracing Using Engineered Rabies Virus Glycoproteins. Cell reports.

Kim J, Zhao T, Petralia RS, Yu Y, Peng H, Myers E, Magee JC (2011) mGRASP enables mapping mammalian synaptic connectivity with light microscopy. Nat Methods 9:96-102.

Langevin C, Tuffereau C (2002) Mutations conferring resistance to neutralization by a soluble form of the neurotrophin receptor (p75NTR) map outside of the known antigenic sites of the rabies virus glycoprotein. Journal of virology 76:10756-10765.

Lentz TL, Burrage TG, Smith AL, Tignor GH (1983) The acetylcholine receptor as a cellular receptor for rabies virus. The Yale journal of biology and medicine 56:315-322.

Li L, Rutlin M, Abraira VE, Cassidy C, Kus L, Gong S, Jankowski MP, Luo W, Heintz N, Koerber HR, Woodbury CJ, Ginty DD (2011) The functional organization of cutaneous low-threshold mechanosensory neurons. Cell 147:1615-1627.

McCoy ES, Taylor-Blake B, Street SE, Pribisko AL, Zheng J, Zylka MJ (2013) Peptidergic CGRPalpha primary sensory neurons encode heat and itch and tonically suppress sensitivity to cold. Neuron 78:138-151.

McNamara CR, Mandel-Brehm J, Bautista DM, Siemens J, Deranian KL, Zhao M, Hayward NJ, Chong JA, Julius D, Moran MM, Fanger CM (2007) TRPA1 mediates formalin-induced pain. Proc Natl Acad Sci U S A 104:13525-13530.

Morimoto K, Hooper DC, Carbaugh H, Fu ZF, Koprowski H, Dietzschold B (1998) Rabies virus quasispecies: implications for pathogenesis. Proc Natl Acad Sci U S A 95:3152-3156.

Muller T, Brohmann H, Pierani A, Heppenstall PA, Lewin GR, Jessell TM, Birchmeier C (2002) The homeodomain factor lbx1 distinguishes two major programs of neuronal differentiation in the dorsal spinal cord. Neuron 34:551-562.

Olausson H, Wessberg J, Morrison I, McGlone F, Vallbo A (2010) The neurophysiology of unmyelinated tactile afferents. Neuroscience and biobehavioral reviews 34:185-191.

Reardon TR, Murray AJ, Turi GF, Wirblich C, Croce KR, Schnell MJ, Jessell TM, Losonczy A (2016) Rabies Virus CVS-N2c(DeltaG) Strain Enhances Retrograde Synaptic Transfer and Neuronal Viability. Neuron 89:711-724.

Ruigrok TJ, van Touw S, Coulon P (2016) Caveats in Transneuronal Tracing with Unmodified Rabies Virus: An Evaluation of Aberrant Results Using a Nearly Perfect Tracing Technique. Frontiers in neural circuits 10:46.

Seidler B, Schmidt A, Mayr U, Nakhai H, Schmid RM, Schneider G, Saur D (2008) A Cre-loxP-based mouse model for conditional somatic gene expression and knockdown in vivo by using avian retroviral vectors. Proc Natl Acad Sci U S A 105:10137-10142.

Sissoeff L, Mousli M, England P, Tuffereau C (2005) Stable trimerization of recombinant rabies virus glycoprotein ectodomain is required for interaction with the p75NTR receptor. The Journal of general virology 86:2543-2552.

Solorzano C, Villafuerte D, Meda K, Cevikbas F, Braz J, Sharif-Naeini R, Juarez-Salinas D, Llewellyn-Smith IJ, Guan Z, Basbaum AI (2015) Primary afferent and spinal cord expression of gastrin-releasing peptide: message, protein, and antibody concerns. J Neurosci 35:648-657.

Sun S, Xu Q, Guo C, Guan Y, Liu Q, Dong X (2017) Leaky Gate Model: Intensity-Dependent Coding of Pain and Itch in the Spinal Cord. Neuron 93:840-853 e845.

Thoulouze MI, Lafage M, Schachner M, Hartmann U, Cremer H, Lafon M (1998) The neural cell adhesion molecule is a receptor for rabies virus. Journal of virology 72:7181-7190.

588 Tuffereau C, Benejean J, Alfonso AM, Flamand A, Fishman MC (1998a) Neuronal cell surface
589 molecules mediate specific binding to rabies virus glycoprotein expressed by a recombinant
590 baculovirus on the surfaces of lepidopteran cells. Journal of virology 72:1085-1091.
591 Tuffereau C, Benejean J, Blondel D, Kieffer B, Flamand A (1998b) Low-affinity nerve-growth factor
592 receptor (P75NTR) can serve as a receptor for rabies virus. Embo J 17:7250-7259.
593 Ugolini G (1995) Specificity of rabies virus as a transneuronal tracer of motor networks: transfer from
594 hypoglossal motoneurons to connected second-order and higher order central nervous
595 system cell groups. J Comp Neurol 356:457-480.
596 Ugolini G (2008) Use of rabies virus as a transneuronal tracer of neuronal connections: implications
597 for the understanding of rabies pathogenesis. Developments in biologicals 131:493-506.
598 Usoskin D, Furlan A, Islam S, Abdo H, Lonnerberg P, Lou D, Hjerling-Leffler J, Haeggstrom J,
599 Kharchenko O, Kharchenko PV, Linnarsson S, Ernfors P (2015) Unbiased classification of
600 sensory neuron types by large-scale single-cell RNA sequencing. Nat Neurosci 18:145-153.
601 Wang H, Zylka MJ (2009) Mrgprd-expressing polymodal nociceptive neurons innervate most known
602 classes of substantia gelatinosa neurons. J Neurosci 29:13202-13209.
603 Wertz A, Trenholm S, Yonehara K, Hillier D, Raics Z, Leinweber M, Szalay G, Ghanem A, Keller G,
604 Rozsa B, Conzelmann KK, Roska B (2015) PRESYNAPTIC NETWORKS. Single-cell-initiated
605 monosynaptic tracing reveals layer-specific cortical network modules. Science 349:70-74.
606 Wickersham IR, Finke S, Conzelmann KK, Callaway EM (2007) Retrograde neuronal tracing with a
607 deletion-mutant rabies virus. Nat Methods 4:47-49.
608 Willoughby RE, Jr., Tieves KS, Hoffman GM, Ghanayem NS, Amlie-Lefond CM, Schwabe MJ, Chusid
609 MJ, Rupprecht CE (2005) Survival after treatment of rabies with induction of coma. The New
610 England journal of medicine 352:2508-2514.
611 Zhang Y, Zhao S, Rodriguez E, Takatoh J, Han BX, Zhou X, Wang F (2015) Identifying local and
612 descending inputs for primary sensory neurons. J Clin Invest 125:3782-3794.
613 Zotterman Y (1939) Touch, pain and tickling: an electro-physiological investigation on cutaneous
614 sensory nerves. J Physiol 95:1-28.

615

616

617

Figure legends

Figure 1. Characterization of the prevalence of neuronal subtypes in lumbar DRGs

(A-D) Immunohistochemical analysis of DRG neurons with antibodies against NeuN, CGRP and NF200 (A), NeuN, TH and IB4 (B), P2X3, PlxnC1 and IB4 (C) and CGRP and TrkA (D). The relative abundance of DRG neurons immunoreactive for the indicated marker(s) is depicted in (E). (F) Schematic representation of which neuron classes are labeled by the antibodies or antibody combinations used in this study. Scale bar: 100μm. Error bars represent the standard deviation

Figure 2. DRG neurons are sensitive to prolonged incubation with SAD ΔG rabies

(A+B) Top row, mCherry (red) expression at 5d (A) and 10d (B) after the injection of SAD.RabiesΔG-mCherry (SAD-G). Bottom row, co-labelling of mCherry and NeuN is depicted (green). (C+D) Immunohistochemical analysis of SAD.RabiesΔG-mCherry infected DRGs with antibodies against mCherry (red) and the macrophage marker IBA1 (cyan) at 5d and 10d post spinal injection. mCherry expression is depicted in the top row, in the bottom row co-labelling of mCherry and IBA1. Note the reduced number of mCherry positive cell bodies at 10d post injection and the strong upregulation of the macrophage marker IBA1. SAD.RabiesΔG-mCherry (SAD-G) was injected intraspinally at $2.4x10^8$ ffu/mL. Scale bar: 100μm

Figure 3. Molecular profiling of SAD.RabiesΔG-eGFP (SAD-G) andSAD.RabiesΔG-mCherry (N2C-G) infected DRG neurons

(A) Schematic representation of the experimental design. SAD-G pseudotyped RabiesΔG-mCherry/eGFP or N2C-G pseudotyped RabiesΔG-mCherry was injected at L3-L5 levels of the lumbar spinal cord of wildtype mice. mCherry/eGFP expression from the rabies genome enables tracing of infected neurons. (B) eGFP expression in a representative image of a lumbar spinal cord section 5 days after infection. Note that infection of local interneurons predominantly occurs in Laminae I-IV. The dotted white line outlines the spinal grey matter. (C-E and G-I) Immunohistochemical analysis of infected DRG neurons with antibodies against NF200, mCherry and TrkA (C and G), with antibodies against P2X3, mCherry and Plxnc1 (D and H) and in (E and I) with antibodies against mCherry and TH. Left column in C-E and G-I shows expression of the indicated markers and the right column depicts the indicated markers together with the rabies derived mCherry. Arrows indicate mCherry+ neurons labeled with two additional markers. Arrowheads indicate mCherry+ neurons labeled with one additional marker. Asterisks indicate mCherry+ neurons that are negative for the analyzed marker. (F and J) Quantification of mCherry+ neurons characterized by the expression of the respective marker after spinal injection of either SAD.RabiesΔG-mCherry (SAD-G) (F) or SAD.RabiesΔG-mCherry (N2C-G) (J). SAD.RabiesΔG-mCherry (SAD-G) and SAD.RabiesΔG-mCherry (N2C-G) were adjusted to the same titer and subsequently injected at $2.4x10^8$ ffu/mL. Scale bars: 100μm. Error bars represent the standard deviation

Figure 4. Evaluation of the activity dependency of rabies virus infection

(A) Schematic representation of the experimental design. SAD-G pseudotyped RabiesΔG-eGFP was injected at L3-L5 levels of the lumbar spinal cord of wildtype mice followed immediately by the injection of formalin into the hindpaw that provides innervation to the spinal injection site. (B) quantification of the percentage of infected DRG neurons in naïve and formalin injected mice. (C-E) Immunhistological stainings with antibodies against GFP, NF200 and TrkA (C), GFP, P2X3 and Plxnc1 (D) and GFP and TH (E). (F) Quantification of the percentage of infected neurons expressing the indicated marker (* = p>0.05). SAD.RabiesΔG-eGFP (SAD-G) was injected at $4.5x10^7$ ffu/mL. Scale bars: 100μm. Error bars represent the standard deviation

Figure 5.Characterization of the molecular identity of DRG expressing Cre in SNS::Cre mice

(A-C) Immunohistochemical analysis of of lumbar DRG neurons in SNS::Cre; $Rosa26^{lsl\text{-}Tomato}$ mice. (A) Analysis of Tomato+ DRG neurons with antibodies against NeuN and TH. (B) Analysis of Tomato+ DRG neurons with antibodies against P2X3 and Plxnc1. (C) Analysis of Tomato+ DRG neurons with antibodies against NF200 and TrkA. (D) Termination zone of Tomato+ primary afferent fibers in the spinal cord is depicted. Dotted lines show the border between LII and LIII and LIII and deeper dorsal horn. (E) Quantification of the proportion of Tomato+ DRG neurons of all DRG neurons (Tom/NeuN) and quantification of the percentage of the indicated markers among all Tomato+ neurons. Scale bar 100μm. Error bars represent the standard deviation

Figure 6. Molecular profiling ofSAD.RabiesΔG-eGFP (Enva) infected DRG neurons from SNS::Cre; $Rosa26^{lsl\text{-}TVA}$ mice

(A) Schematic representation of the experimental design. SAD.RabiesΔG-eGFP (Enva) contains the same genome as SAD.RabiesΔG-eGFP (SAD-G) but is pseupotyped with the EnvA glycoprotein instead. SAD.RabiesΔG-eGFP (Enva)was injected into L3-L4 levels of the lumbar spinal cord of SNS::Cre; $Rosa26^{lsl\text{-}TVA}$ mice. (B) Characerization of eGFP+ neurons with antibodies directed against NF200 and TrkA. (C) Detection of a P2X3+;Plxnc1+ infected DRG neuron (eGFP+). (D) Analysis of infected DRGs with antibodies against GFP and TH. Arrows indicate eGFP+ neurons labeled with two additional markers. Asterisks indicate eGFP+ neurons that are negative for the analyzed marker. (E) Quantification of the percentage of eGFP+ expressing the indicated marker. SAD.RabiesΔG-eGFP (Enva) was injected at $3.5x\ 10^8$ ffu/mL. Scale bars: 100μm. Error bars represent the standard deviation

Figure 7. Monosynaptic tracing initiated from spinal Grp::Cre neurons

(A and A') Grp::Cre neurons are located in lamina II of the spinal cord. The neuropil and cell bodies of GRP::Cre neurons overlap with central terminals of IB4+ and TH+ primary afferent fibers. (B) High resolution imaging of a tdTomato+ Grp neuron (red) indicates the presence of Homer1+ (green) postsynapses on Grp neurons which are in close proximity to IB4+ (blue) terminals. (C) High resolution imaging of tdTomato+ Grp neuropil (red) indicates the presence of Homer1+ (blue)

postsynapses on Grp neurons in close proximity to vGlut3+ (green) primary afferent terminals. (D) Rabies mediated monosynaptic retrograde tracing reveals many primary (mCherry+ and eGFP+) and secondary (only eGFP+) infected spinal neurons. (E) Secondary infected DRG neurons are mostly NF200+ (arrows). (F) Quantification of eGFP labelled DRG neuron subtypes after retrograde transduction mediated by either SAD-G or oG rabies glycoprotein. SAD.RabiesΔG-eGFP (Enva) was always injected at 3.5x 10^8 ffu/mL. AAV1.EF1a.flex.mCherry-2A-SADG and pAAV1.Ef1a.DIO.oG.WPRE.hGH were injected at 9.5x 10^{12} GC/mL Scale bars: 100μm (A, D, E) 5μm (B, C). Error bars represent the standard deviation

Figure 8. Monosynaptic retrograde tracing is limited to subsets of sensory neurons.

The dorsal spinal horn is innervated by myelinated and unmyelinated primary afferent fibers (myelinated = Aβ-fibers and Aδ-fibers from NF and PEP neurons, unmyelinated = C-fibers from non-peptidergic (NP), peptidergic (PEP) and C-LTMRs (TH)). G-deleted rabies virus pseudotyped with the rabies glycoproteins SAD19B-G or N2C-G are largely restricted from entering central terminals of NP and TH neurons. Central terminals of NP neurons show some limited susceptibility to infection with G-deleted rabies virus pseudotyped with the optimized rabies glycoprotein (oG).

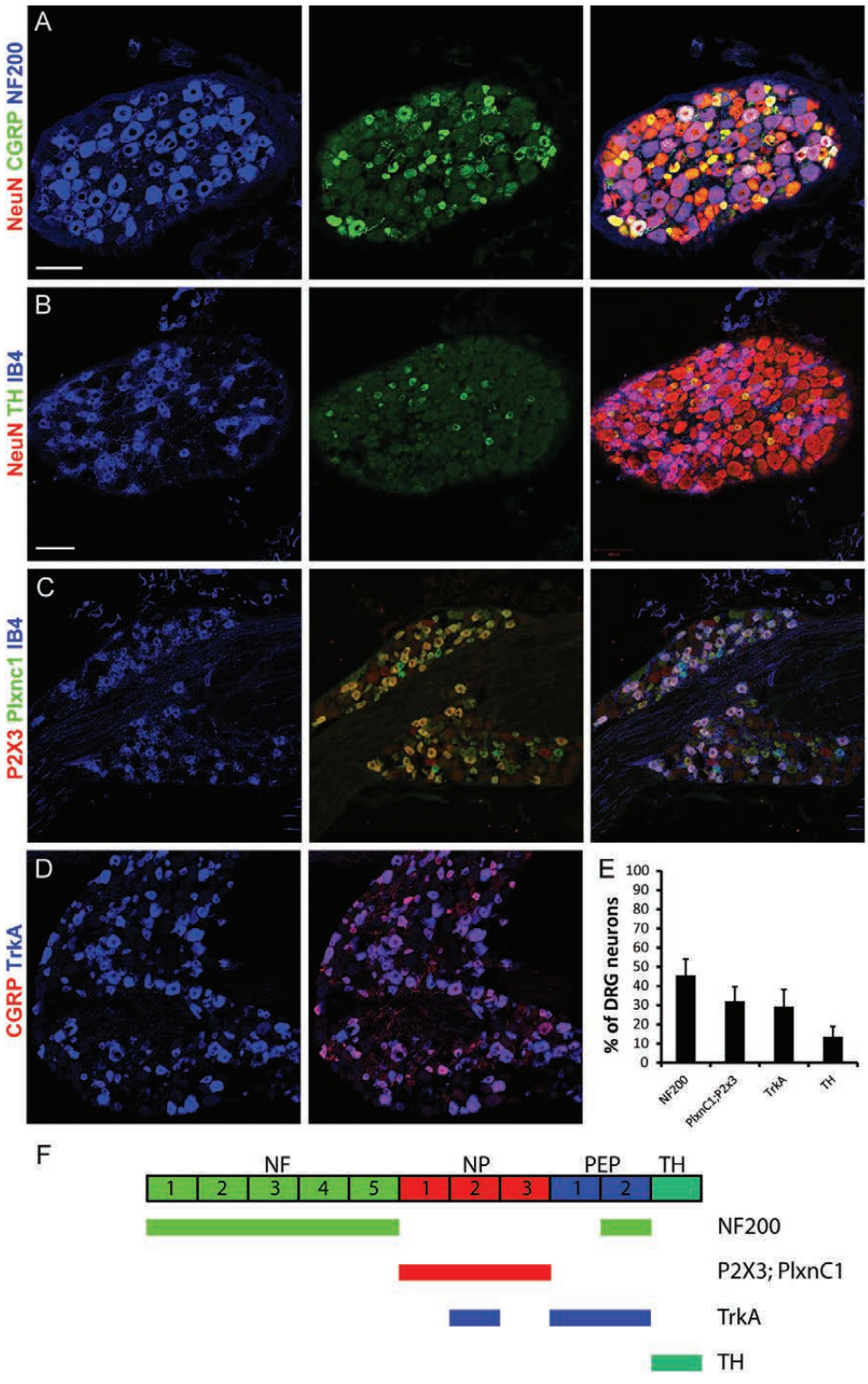

Figure 1

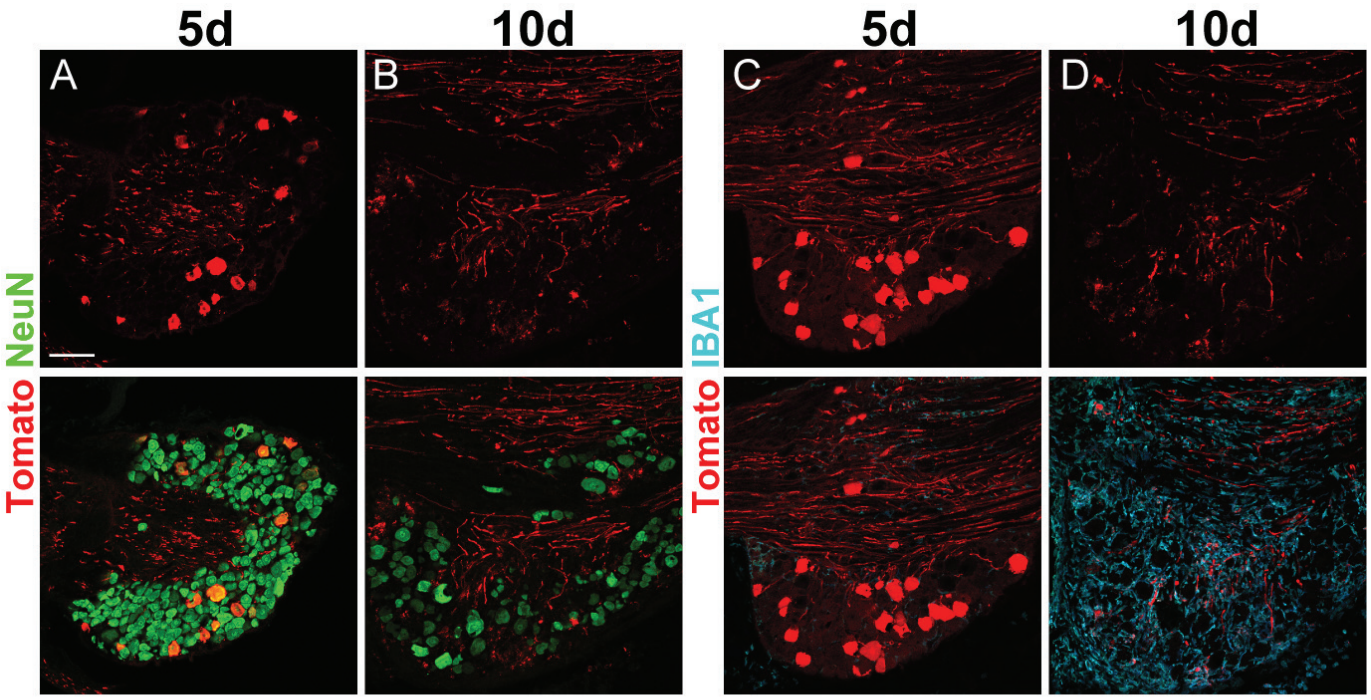

Figure 2

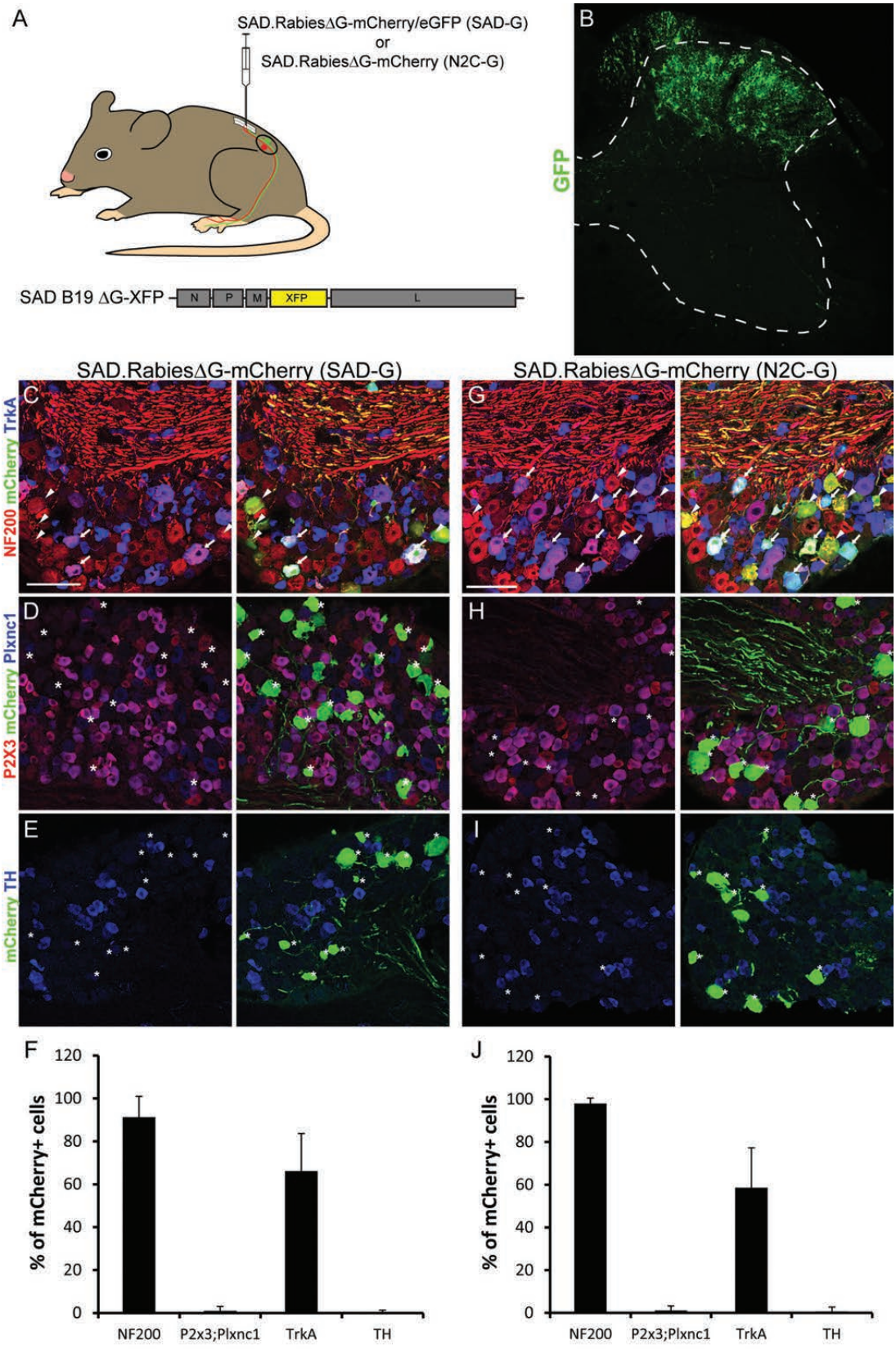

Figure 3

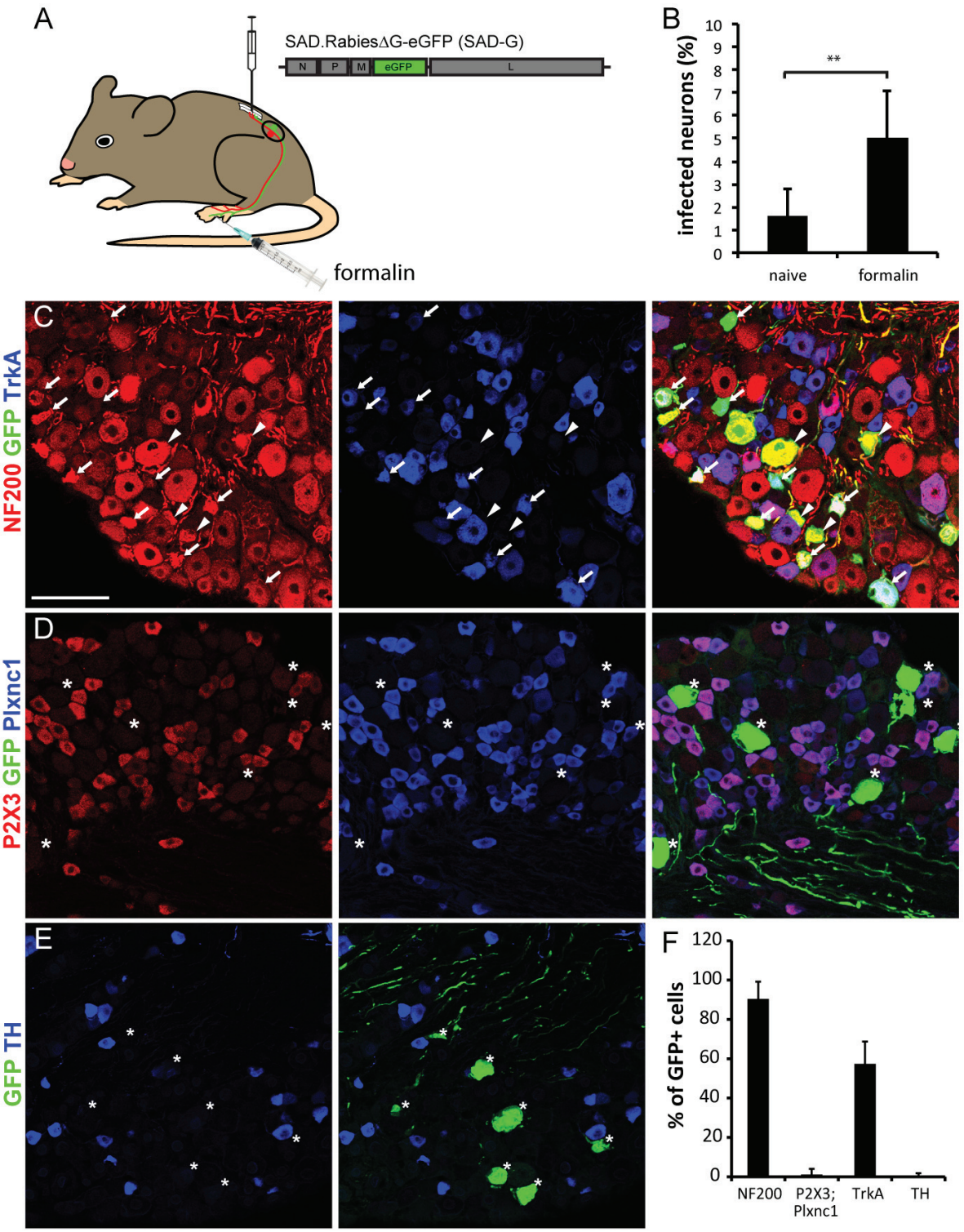

Figure 4

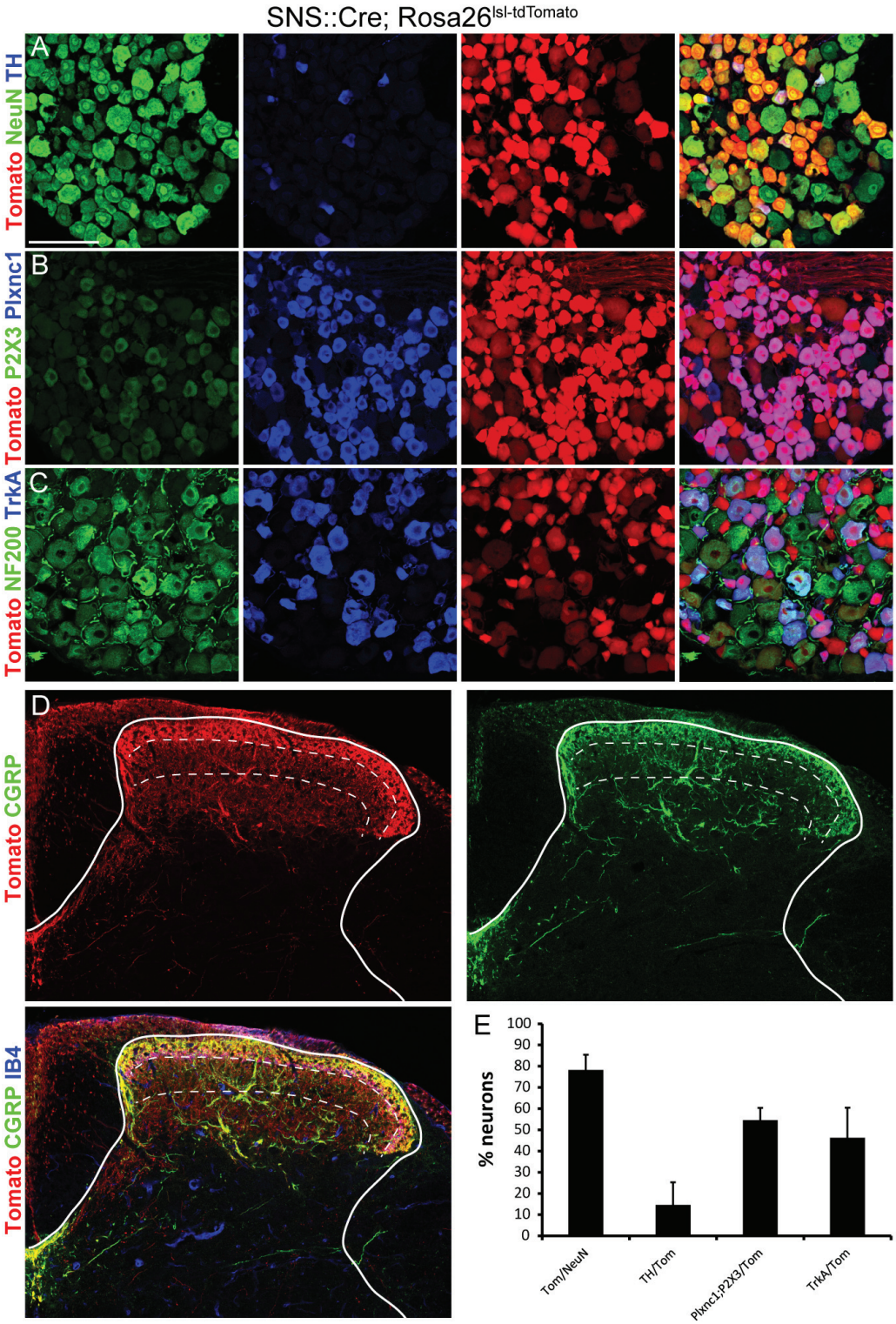

Figure 5

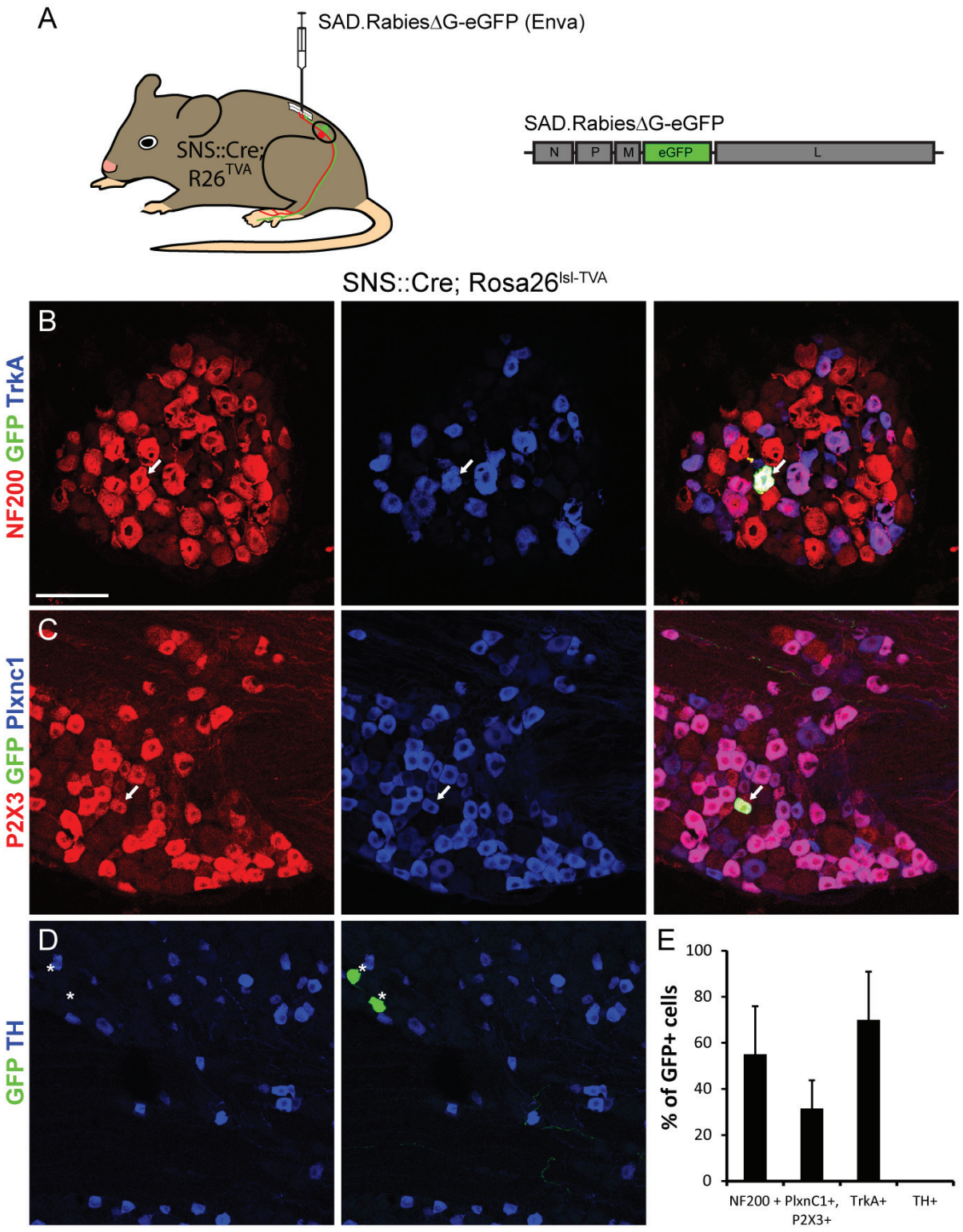

Figure 6

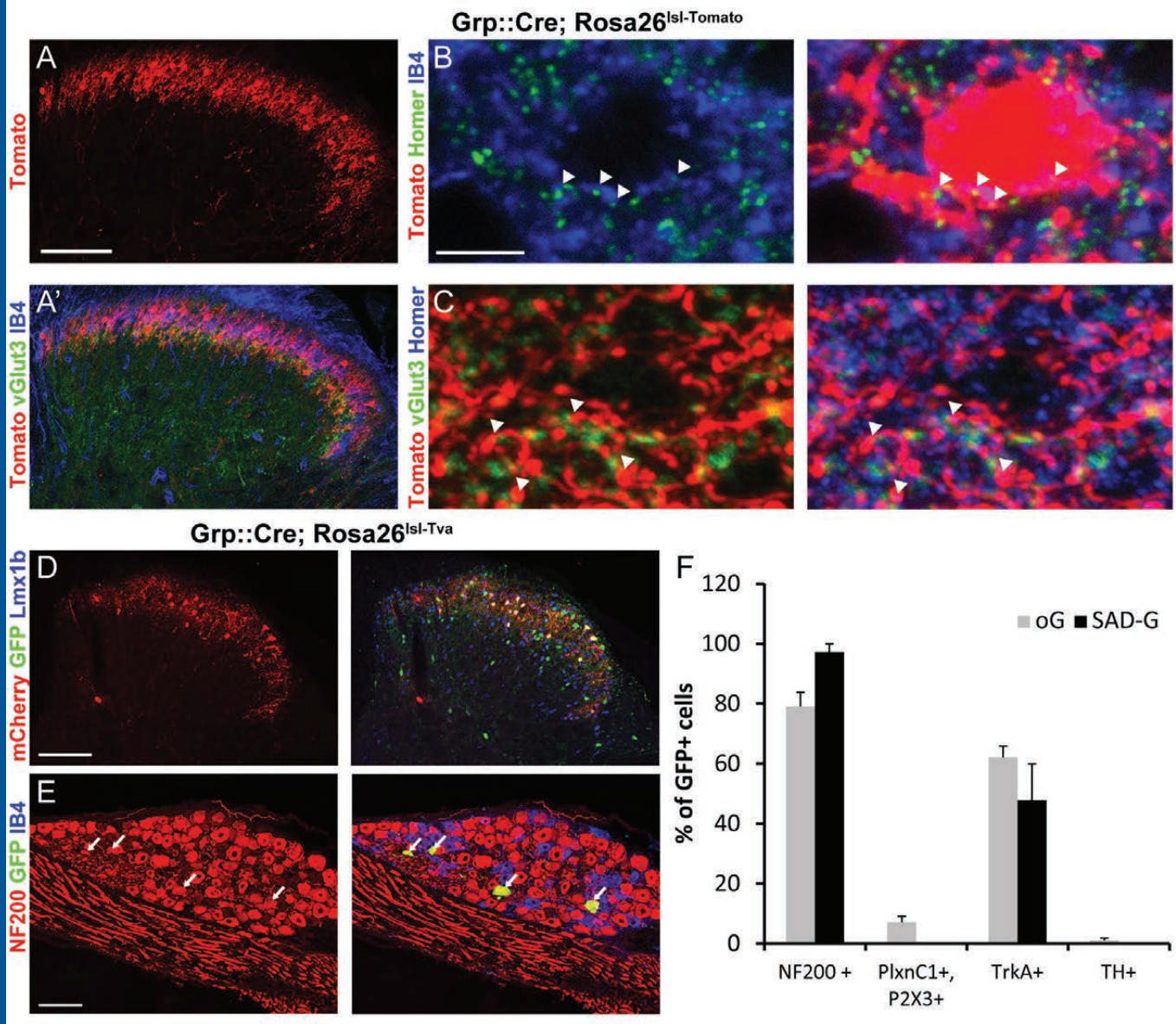

Figure 7

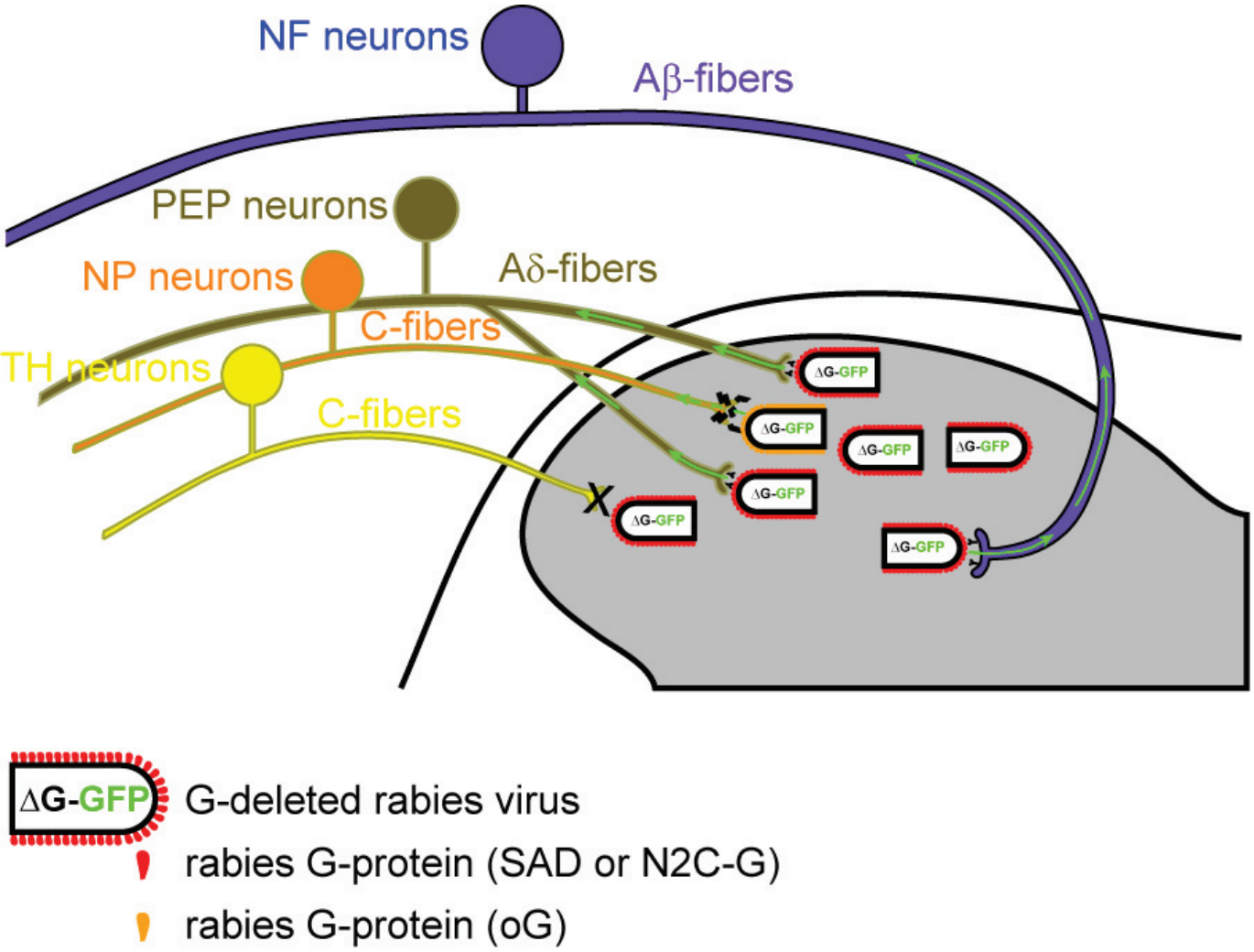

Figure 8

gene	NF					NP			PEP		TH
	NF1	NF2	NF3	NF4	NF5	NP1	NP2	NP3	PEP1	PEP2	TH
Ncam1	6.5	0	0	4.5	0	32.8	31.3	16.7	28.1	11.7	55.8
Ncam2	13	8.3	25	0	3.8	1.6	3.1	0	7.8	41.2	1.3
Chrna1	0	6.3	33.3	0	0	0	0	0	0	0	0.4
Chrna10	0	0	8.3	0	0	0	0	0	0	17.6	0
Chrna2	0	0	0	0	0	0.8	0	0	0	0	0
Chrna3	0	2.1	0	0	0	0	0	0	1.6	17.6	0
Chrna4	0	2.1	0	0	0	0	0	8.3	0	0	14.6
Chrna5	0	2.1	0	0	3.8	0	0	0	0	0	0
Chrna6	35.5	2.1	0	0	0	32	31.3	41.7	12.5	0	1.7
Chrna7	0	4.2	16.7	0	3.8	0.8	0	0	1.6	11.8	0
Chrna9	0	0	0	0	0	0	0	0	0	0	0
Chrnb1	0	0	0	0	0	1.6	0	0	3.1	0	0.5
Chrnb2	38.7	27.1	58.3	9.1	34.6	35.2	9.4	8.3	6.3	23.5	18.9
Chrnb3	0	0	0	0	0	4.8	0	0	7.8	0	0.5
Chrnb4	0	0	0	0	0	0.8	0	0	3.1	11.8	0
Chrnd	0	0	0	4.5	3.8	0	3.1	0	0	5.9	0
Chrne	0	0	0	0	0	0	0	0	0	0	0
Chrng	0	0	0	0	3.8	0.8	0	0	0	0	0
Ngfr	90.3	70.9	100	18.2	42.3	1.6	31.3	0	42.2	100	46.8

Table 1: Expression of known rabies receptors in DRG subpopulations

First column indicates gene name. The headers of columns 2-12 indicate the respective class (top row) and subpopulation (second row) of DRG neurons. Numerical values indicate the fraction of positive cells (%) for different neuronal populations. Data was extracted from http://linnarssonlab.org/drg/ (External resource Table 2).